Supporting Information for

Redox Active Ni-Pd Carbonyl Alloy Nanoclusters: Syntheses, Molecular Structures and Electrochemistry of $[Ni_{22-x}Pd_{20+x}(CO)_{48}]^{6-}$ (x = 0.62), $[Ni_{29-x}Pd_{6+x}(CO)_{42}]^{6-}$ (x = 0.09) and $[Ni_{29+x}Pd_{6-x}(CO)_{42}]^{6-}$ (x = 0.27)

Beatrice Berti,[a] Cristiana Cesari,[a] Cristina Femoni,[a] Tiziana Funaioli,[b] Maria Carmela Iapalucci[a] and Stefano Zacchini[a]*

[a] Dipartimento di Chimica Industriale "Toso Montanari", Università di Bologna, Viale Risorgimento 4, 40136 Bologna. Italy. E-mail: stefano.zacchini@unibo.it

[b] Dipartimento di Chimica e Chimica Industriale, Università di Pisa, Via G. Moruzzi 13, 56124, Pisa, Italy
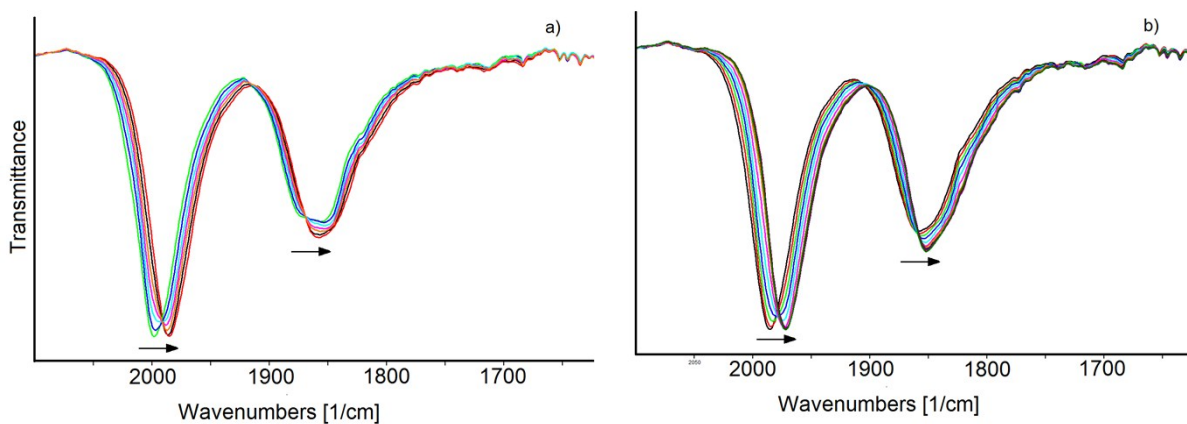
Figure S1. IR spectral changes of a CH₃CN solution of [**1**]$^{6-}$ recorded in an OTTLE cell during the progressive decrease of the potential from: (a) -0.8 to -1.2 V; (b) -1.2 to -1.5 V *vs*. Ag pseudo-reference electrode (scan rate 1 mV s^{-1}). [N^{n}Bu$_4$][PF$_6$] (0.1 mol dm^{-3}) as the supporting electrolyte. The absorptions of the solvent and the supporting electrolyte have been subtracted.
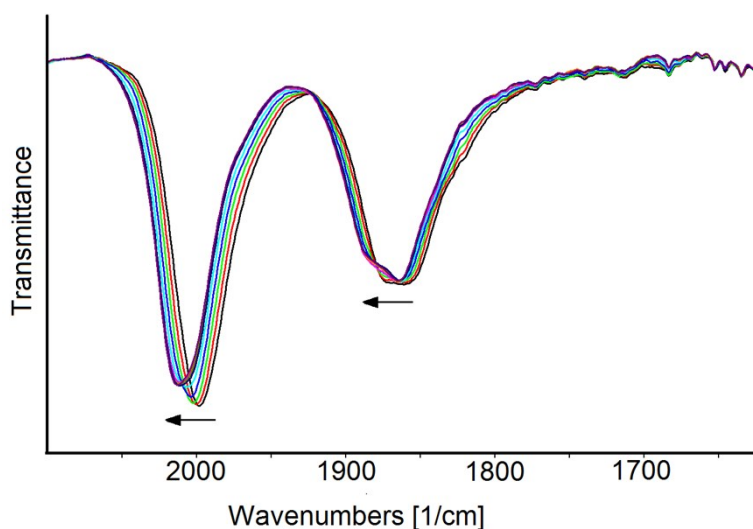

Figure S2. IR spectral changes of a CH₃CN solution of [**1**]$^{6-}$ recorded in an OTTLE cell during the progressive increase of the potential from -0.3 to 0.0 V *vs*. Ag pseudo-reference electrode (scan rate 1 mV s^{-1}). [N^{n}Bu$_4$][PF$_6$] (0.1 mol dm^{-3}) as the supporting electrolyte. The absorptions of the solvent and the supporting electrolyte have been subtracted.

Figure S3. DPV and CV profiles recorded at Pt electrode in CH$_3$CN solution of [**2**]$^{6-}$. [N^{n}Bu$_4$][PF$_6$] (0.1 mol dm^{-3}) supporting electrolyte. Scan rate for CV: 0.1 V s^{-1}.

Figure S4. IR spectral changes of a CH$_3$CN solution of [**2**]$^{6-}$ recorded in an OTTLE cell during the progressive sweep of the potential from: (a) -0.6 to -1.2 V ; (b) -1.2 to -1.5 V; (c) -1.5 to -1.8 V; (d) -0.6 to +0.2 V *vs*. Ag pseudo-reference electrode (scan rate 0.5 mV s^{-1}). [N^{n}Bu$_4$][PF$_6$] (0.1 mol dm^{-3}) as the supporting electrolyte. The absorptions of the solvent and the supporting electrolyte have been subtracted.
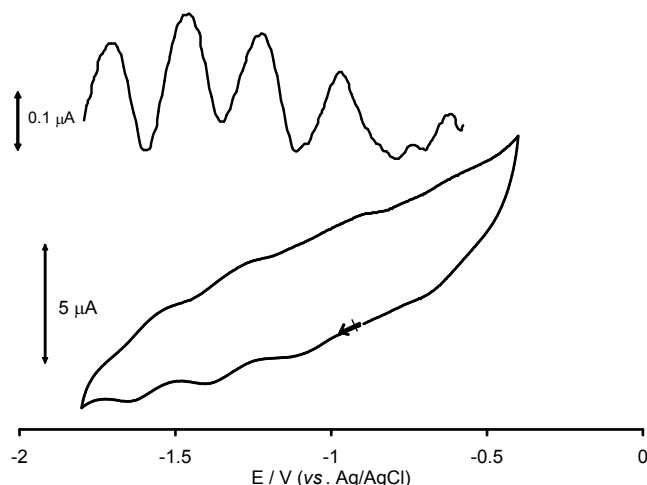
Figure S5. Comparison of the IR spectra in the ν_{CO} region of the CH_3CN solution of $[2]^{6-}$ recorded in an OTTLE cell: (red line) starting solution before oxidation; (black line) the potential has been restored to the initial value (-0.6 V *vs*. Ag pseudo-reference) after the oxidation step of Figure S4(d) (-0.6 to +0.2 V *vs*. Ag pseudo-reference electrode, scan rate 0.5 mV s^{-1}). [N^{n}Bu$_4$][PF$_6$] (0.1 mol dm^{-3}) as the supporting electrolyte. The absorptions of the solvent and the supporting electrolyte have been subtracted.
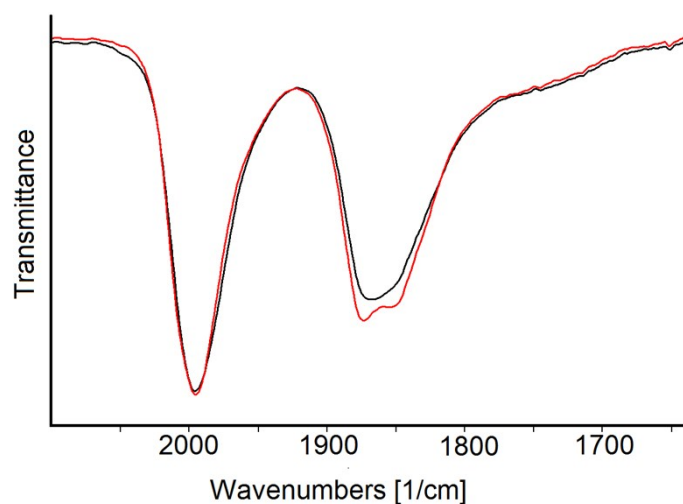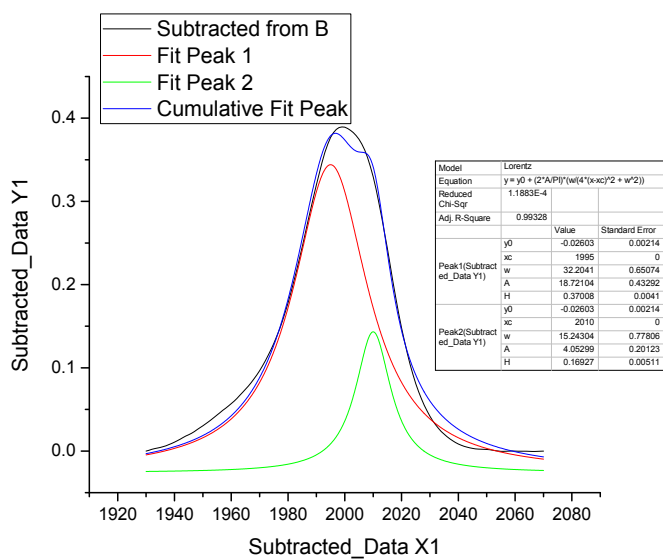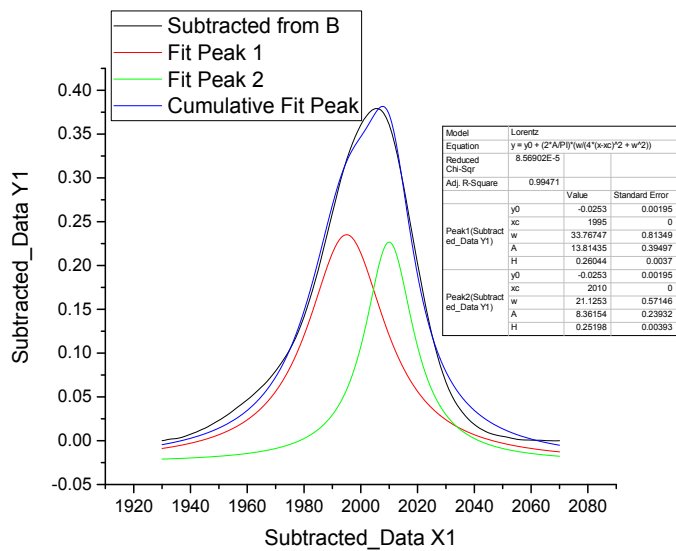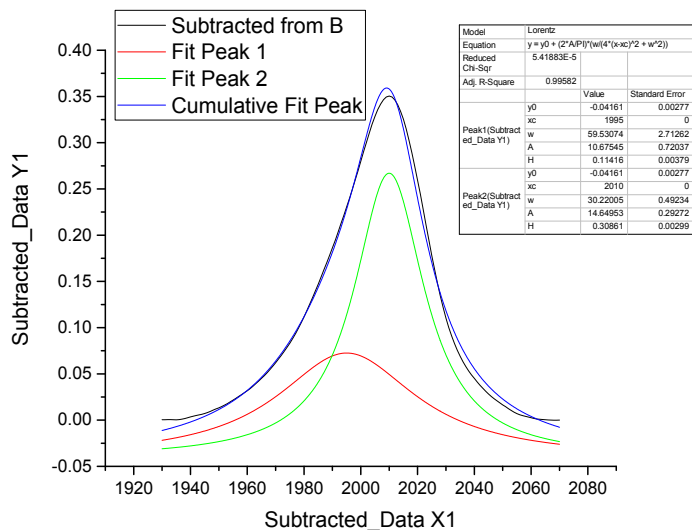
Plot 1

Model	Lorentz	
Equation	y = y0 + (2*A/PI)*(w/(4*(x-xc)^2 + w^2))	
Reduced Chi-Sqr	5.41883E-5	
Adj. R-Square	0.99582	
	Value	Standard Error
y0	-0.04161	0.00277
xc	1995	0
Peak1(Subtracted_Data Y1) w	59.53074	2.71262
A	10.67545	0.72037
H	0.11416	0.00379
y0	-0.04161	0.00277
xc	2010	0
Peak2(Subtracted_Data Y1) w	30.22005	0.49234
A	14.64953	0.29272
H	0.30861	0.00299

Plot 2

Model	Lorentz	
Equation	y = y0 + (2*A/PI)*(w/(4*(x-xc)^2 + w^2))	
Reduced Chi-Sqr	8.56902E-5	
Adj. R-Square	0.99471	
	Value	Standard Error
y0	-0.0253	0.00195
xc	1995	0
Peak1(Subtracted_Data Y1) w	33.76747	0.81349
A	13.81435	0.39497
H	0.26044	0.0037
y0	-0.0253	0.00195
xc	2010	0
Peak2(Subtracted_Data Y1) w	21.1253	0.57146
A	8.36154	0.23932
H	0.25198	0.00393

Plot 3

Model	Lorentz	
Equation	y = y0 + (2*A/PI)*(w/(4*(x-xc)^2 + w^2))	
Reduced Chi-Sqr	1.1883E-4	
Adj. R-Square	0.99328	
	Value	Standard Error
y0	-0.02603	0.00214
xc	1995	0
Peak1(Subtracted_Data Y1) w	32.2041	0.65074
A	18.72104	0.43292
H	0.37008	0.0041
y0	-0.02603	0.00214
xc	2010	0
Peak2(Subtracted_Data Y1) w	15.24304	0.77806
A	4.05299	0.20123
H	0.16927	0.00511

Figure S6. Peak fitting analysis of three spectra acquired during the oxidation of [**2**]$^{6-}$.

Table S1

Crystal data and experimental details for [NBu$_4$]$_6$[**1**]·4CH$_3$COCH$_3$, [NEt$_4$]$_6$[**2**]·3CH$_3$CN·solv and [NEt$_4$]$_6$[**3**]·3CH$_3$CN·solv.

	[NBu$_4$]$_6$[**1**]·4CH$_3$COCH$_3$	[NEt$_4$]$_6$[**2**]·3CH$_3$CN·solv	[NEt$_4$]$_6$[**3**]·3CH$_3$CN·solv
Formula	C$_{156}$H$_{240}$N$_6$Ni$_{21.37}$O$_{52}$Pd$_{20.63}$	C$_{95}$H$_{129}$N$_9$Ni$_{28.91}$O$_{42}$Pd$_{6.09}$	C$_{95}$H$_{129}$N$_9$Ni$_{29.27}$O$_{42}$Pd$_{5.73}$
Fw	6481.19	4414.11	4409.19
T, K	100(2)	100(2)	100(2)
λ, Å	0.71073	0.71073	0.71073
Crystal system	Monoclinic	Trigonal	Trigonal
Space Group	$C2/c$	$P\bar{3}1c$	$P\bar{3}1c$
a, Å	38.6411(12)	18.0295(15)	18.0130(14)
b, Å	17.6379(6)	18.0295(15)	18.0130(14)
c, Å	33.0067(17)	23.386(2)	23.2710(17)
α, °	90	90	90
β, °	119.3140(10)	90	90
γ, °	90	120	120
Cell Volume, Å^3	19615.1(14)	6583.6(12)	6539.1(11)
Z	4	2	2
D$_c$, g cm^{-3}	2.195	2.227	2.239
μ, mm^{-1}	3.902	4.903	4.939
F(000)	12725	4375	4374
Crystal size, mm	0.21×0.16×0.14	0.22×0.18×0.14	0.21×0.16×0.15
θ limits, °	1.692–27.000	2.176–25.045	2.261–25.047
Index ranges	-49≤ h ≤49 -22≤ k ≤22 -42≤ l ≤40	-21≤ h ≤21 -21≤ k ≤21 -27≤ l ≤27	-21≤ h ≤21 -21≤ k ≤21 -27≤ l ≤27
Reflections collected	149731	103805	103697
Independent reflections	21214 [R$_{int}$ = 0.0510]	3889 [R$_{int}$ = 0.0957]	3870 [R$_{int}$ = 0.0768]
Completeness to θ max	99.6%	99.5%	99.7%
Data / restraints / parameters	21214 / 445 / 1129	3889 / 178 / 293	3870 / 178 / 293
Goodness on fit on F^2	1.061	1.212	1.089
R$_1$ (I > 2σ(I))	0.0452	0.1011	0.0988
wR$_2$ (all data)	0.1033	0.2390	0.2793
Largest diff. peak and hole, e Å^{-3}	3.595 / −1.211	1.660 / −1.159	2.247 / −1.792